2016 IEEE/RSJ International Conference on Intelligent Robots and Systems (IROS)
Daejeon Convention Center
October 9-14, 2016, Daejeon, Korea

Design and Modeling of a Compact Rotational Nonlinear Spring

Hamed Jalaly Bidgoly[1] and Majid Nili Ahmadabadi[1] and Mohammad Reza Zakerzadeh[2]

Abstract— **In this paper, we propose a new method for implementing a rotational nonlinear spring with user defined profile, based on the combination of a linear spring with a nonlinear transmission mechanism. The proposed structure consists of a non-circular cam, a roller which moves along outer circumference of the cam, and a stretched translational linear spring which is connected between center of the cam and center of the roller. We obtain a set of differential equations to design shape of the cam for any given torque-angle profile. Also, it will be shown that profiles with both positive and negative values can be implemented by the proposed method. At last, the cam of some popular nonlinear springs are designed, including constant, cubic, hyperbolic tangent and sinusoidal springs.**

I. Introduction

In recent years, springs are widely used in robotics. They can be used as a low-pass filter to absorb impact forces for safe collision and safe human-robot interactions[1]. They can produce a passive torque to compensate gravity and reduce actuator torque in the balancing conditions[2]. Series springs with actuators, namely series elastic actuator, convert the difficult problem of force control to the simple problem of position control and also filter effects of load perturbations on the actuator[3]. Parallel springs with actuators modify the natural dynamics of robots and provide some part of the actuator torque[4] and simply control task[5]. In the quadruped robots, using springs in the legs and spine improves the stability[6], reduces energy consumption[7] and simplifies the control task[8]. In cyclic tasks with consecutive joints accelerations and decelerations, springs can prevent energy dissipation by storing mechanical energy during deceleration phase as potential energy and releasing it during acceleration phase[9].

Generally, both linear and nonlinear springs are used in robotics; however, it has been shown that nonlinear springs result in better performance in the mentioned applications such as safe collision and shock absorption[10] or weight compensation[11], [12]. The nonlinear spring enhances the stability of passive dynamic running[13], increases link velocity[14] and leads to faster and more stable locomotion[15]. The nonlinear spring in series with the actuator, enables independent control of both joint angle and joint stiffness[16] and in parallel with actuator, efficiently minimizes the actuator torque[17]. Also, there are biological evidences that show muscle-tendon tissues have nonlinear stiffness[18]. Moreover, the nonlinear springs are used in other non-robotics applications such as vibration damping[19] and shock protection in MEMS[20].

So far, there are two main approaches to implement nonlinear spring. In the first approach, morphology of a compliant structure is designed in such a way that it exposes nonlinear behaviour. This approach covers from simple methods such as making some lateral slits in a bar[21] or connecting two bent metal sheets[22], to complex ones such as designing topology of a branching network of compliant beams[23] or optimizing topology of a compliant bar[24]. In the second approach, a linear spring is connected to a nonlinear transmission mechanism. This approach, itself, can be categorized in two groups. In the first group, a stretched spring is connected to a cable where wraps around a non-circular pulley[11], [12], [25]. In these structures, the linear rotation of the pulley causes nonlinear changes of spring length. In the second group, the spring directly moves between or around some other parts with uncommon nonlinear geometry[14], [16], [26] where again results in nonlinear changes of spring length.

Although the first approach requires less mechanical parts and it's more compact, implementation of the second approach is more straightforward and can be easily realized by off-the-shell linear springs. Also the first group, in the second approach, can only provide uni-directional torque, since the cable can just be pulled. Therefore, two antagonistic nonlinear springs should be used to provide bi-directional torque with both positive and negative values. This itself increases the mass and size of the whole structure.

In this paper, a new method to implement the nonlinear rotational spring, based on the motion of a linear spring along outer circumference of a non-circular cam, is proposed. This method belongs to the second group from the second approach mentioned above. Here, our main concern is the implementation of a compact nonlinear rotational spring, capable of providing both positive and negative user defined torques with just one single structure rather than combination of two antagonistic structures. Compared with the other methods in this group, the motion range of proposed structure in [14] is too restricted. Also, in [16], [26], just translational nonlinear spring are implemented. The rest of the paper is organized as follows; in Section II, the proposed method is described and dynamics and simplified static models of the proposed structure are derived. Implementation of different nonlinear profiles are addressed in Section III. Finally, we conclude this paper and discuss future works in Section IV.

[1]H. J. Bidgoly and M. N. Ahmadabadi are with Cognitive Robotics Laboratory, The Control and Intelligent Processing Center of Excellence (CIPCE), School of Electrical and Computer Engineering, College of Engineering, University of Tehran, Tehran, Iran (jalaly.hamed@ut.ac.ir; mnili@ut.ac.ir).

[2]M. R. Zakerzadeh is with Dynamic and Vibration Laboratory, School of Mechanical Engineering, College of Engineering, University of Tehran, Tehran, Iran (zakerzadeh@ut.ac.ir).

II. Synthesis of the Proposed Nonlinear Rotational Spring

Consider a non-circular cam with a stretched linear spring, that one of its sides is hinged to the center of cam and the other side of spring is attached to a roller. The roller moves along outer circumference of the cam through a radial non-flexible guide. Both the spring guide and the roller rotate along joint axis and the cam is fixed. Schematic of the proposed structure is illustrated in Fig. 1.

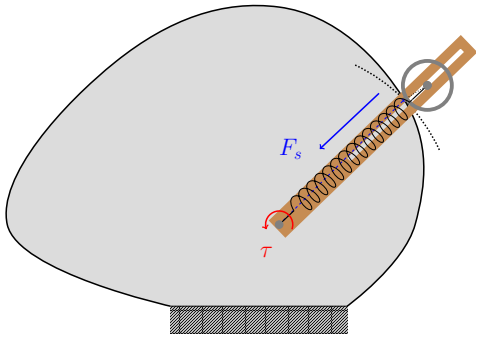

Fig. 1. Schematic of nonlinear rotational spring

In Fig. 1, τ is external torque applied to the guide around the rotation axis of spring and F_s is spring force in the radial direction. Because of the non-circular shape of the cam, the normal direction to the cam is not in the radial direction; so, tangential component of the spring force causes a motion in a direction where the spring length decreases. On the other hand, the external torque τ, if applied in an opposite direction, causes a motion in a direction where the spring length increases. Consequently, each torque resists against the other one and if they are equal, the system reaches balance condition. The resulted torque from the tangential component of the spring force, is dependent on the length of the spring and the angle between normal and radial direction. Therefore, one can design the shape of cam in order to create specific torque at each position and consequently, realize any smooth torque-angle profile. In the following section, we explain the procedure to design the shape of cam for any given torque-angle profile by first modeling the dynamics of structure and then simplifying the model. Currently, it is assumed that the guide and spring are massless and the spring is ideal.

A. Dynamic Model

To model the dynamics of the structure, the free-body diagrams of guide and roller are shown in Fig. 2 and Fig. 3, respectively. In Fig. 2, τ is the desired torque, F_1 is the exerted force by the roller on the guide and l is radial distance between the axis of rotation and the centre of the roller which is length of spring. If mass of the guide is negligible, the Euler equation can be written as the following equation:

$$\tau(\theta_s) = -F_1 \,.\, l(\theta_s). \tag{1}$$

In Fig. 2, l is again the length of the spring and r is the radius of the cam in contact point. Also, α is the angle between lines from the rotation axis to the center of roller and the contact point. ϕ is the angle between the normal force and extension of contact line. F_s is the spring force which equals to:

$$F_s(\theta_s) \;=\; K(l(\theta_s) - l_0), \tag{2}$$

where l_0 is rest length of spring and K is its constant. In this figure, F_2 is reaction force of the guide to the roller which by the assumption of massless guide, it results in a torque equivalent to the applied torque τ. f_f is friction force between the roller and the circumference of the cam at the contact point. Finally, N is the normal force, exerted on the contact point. Considering Newton-Euler equations, dynamics of roller can be written as:

$$-F_s + N\cos(\phi-\alpha) - f_f \sin(\phi-\alpha) = m\, a_{_R} = m(\ddot{l} - l\dot{\theta}_s^2), \tag{3}$$

$$F_2 - N\sin(\phi-\alpha) - f_f \cos(\phi-\alpha) = m\, a_{_\theta} = m(l\ddot{\theta}_s + 2\dot{l}\dot{\theta}_s) \tag{4}$$

$$f_f\, R = I\, \dot{\omega} \tag{5}$$

where $a_{_R}$ is radial acceleration, $a_{_\theta}$ is azimuthal acceleration and R, m and I are the radius, the mass and the inertia momentum of roller, respectively. Moreover, the spring force causes the roller to be permanently in touch with the cam which exposes a geometrical soft constraint on the motion direction. As illustrated in Fig. 4, the motion direction always has an angle of $\phi - \alpha$ with respect to the radial direction which can be expressed easily with the velocity vector in the *intrinsic coordinates* as:

$$\underline{v} \;=\; \nu\, \hat{e}_{_t}, \tag{6}$$

where ν is tangential velocity of the roller center. On the other hand, the velocity vector can also be expressed in the *polar coordinates* as:

$$\underline{v} \;=\; v_{_R}\hat{e}_{_R} + v_{_\theta}\hat{e}_{_\theta} \;=\; \dot{l}\hat{e}_{_R} \;+\; l\dot{\theta}_s\hat{e}_{_\theta}, \tag{7}$$

where $v_{_R}$ is radial velocity and $v_{_\theta}$ is azimuthal velocity. One can simply show that the mentioned constraint on the motion makes the radial and the azimuthal velocities dependent on each other as following:

$$\tan(\phi - \alpha) \;=\; \frac{v_{_R}}{v_{_\theta}} \;=\; \frac{\dot{l}}{l\,\dot{\theta}_s}\,. \tag{8}$$

It should be noted that, this constraint is still geometrically valid for zero velocity, where $\dot{\theta} = 0$, by evaluating the indeterminate form $0/0$:

$$\tan(\phi - \alpha) \;=\; \frac{\mathrm{d}l}{l\,\mathrm{d}\theta_s}\,.$$

To determine ω and $\dot{\omega}$, and consequently f_f, it is assumed that rolling is without slipping which yields:

$$R\omega = \nu \Rightarrow R\,\dot{\omega} = \dot{\nu}, \tag{9}$$

where $\dot{\nu}$ is tangential acceleration of the roller center. It can be calculated by describing the acceleration vector in both

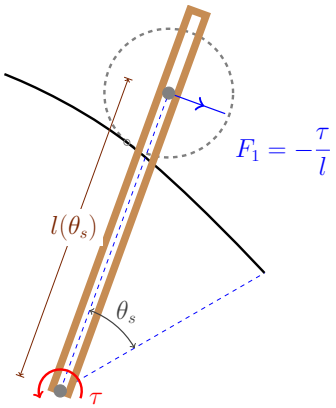

Fig. 2. Free-body diagram of the guide. τ is external torque and F_1 is force exerted by roller.

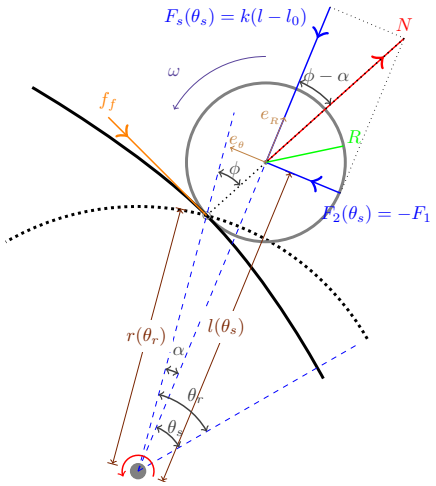

Fig. 3. Free-body diagram of the roller.

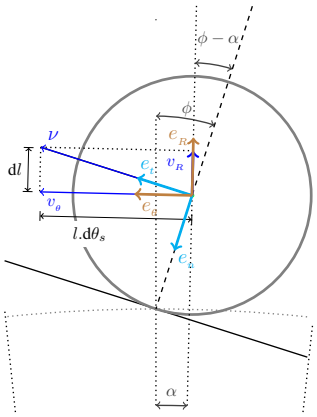

Fig. 4. Differential relation between dl, dθ_s and $\phi - \alpha$.

of *intrinsic coordinates* and *polar coordinates*:

$$\begin{cases} \underline{a} = \dot{\nu}\hat{e}_t + \dfrac{\nu^2}{\rho}\hat{e}_n, \\ \underline{a} = a_R\hat{e}_R + a_\theta\hat{e}_\theta. \end{cases}$$

Equalling both of equations and decomposing unit vectors of polar coordinates over unit vectors of intrinsic coordinates, yields:

$$\begin{aligned} \dot{\nu} &= a_R \sin(\phi-\alpha) + a_\theta \cos(\phi-\alpha) \\ &= (\ddot{l} - l\dot{\theta}_s^2)\sin(\phi-\alpha) + (l\ddot{\theta}_s + 2\dot{l}\dot{\theta}_s)\cos(\phi-\alpha). \end{aligned} \tag{10}$$

The no slipping condition is valid if the calculated f_f is less than $\mu_s N$, where μ_s is the coefficient of static friction; otherwise, the friction force is calculated by $f_f = \mu_k N$ where μ_k is the coefficient of kinetic friction, and the motion of roller includes both rolling and slipping.

To find the relation between l and τ, we first eliminate N between (3) and (4):

$$\begin{aligned} &-F_s\sin(\phi-\alpha) + F_2\cos(\phi-\alpha) - f_f = \\ &\quad m(\ddot{l} - l\dot{\theta}_s^2)\sin(\phi-\alpha) + m(l\ddot{\theta}_s + 2\dot{l}\dot{\theta}_s)\cos(\phi-\alpha). \end{aligned} \tag{11}$$

Then, f_f is substituted by considering (5), (9) and (10):

$$\begin{aligned} &-F_s\sin(\phi-\alpha) + F_2\cos(\phi-\alpha) = \\ &\quad \frac{3}{2}m\Big((\ddot{l} - l\dot{\theta}_s^2)\sin(\phi-\alpha) + (l\ddot{\theta}_s + 2\dot{l}\dot{\theta}_s)\cos(\phi-\alpha)\Big). \end{aligned} \tag{12}$$

Finally, by substituting F_s, F_2 and $\tan(\phi-\alpha)$, we have:

$$-K(l-l_0)\dot{l} + \tau\,\dot{\theta}_s = \frac{3}{2}m\left(\ddot{l}\dot{l} + l^2\,\dot{\theta}_s\ddot{\theta}_s + l\,\dot{l}\dot{\theta}_s^2\right). \tag{13}$$

In the last differential equation, $l(\theta_s = 0)$, l_0 and K are design parameters, τ and profile of θ_s are assumed to be known and given by the user and the profile of l is unknown. Although this differential equation is too nonlinear, it can be numerically solved by following first order ordinary differential equations:

$$\begin{cases} \dot{x}_1 = x_2, \\ \dot{x}_2 = \dfrac{\left(\frac{2}{3m}\left(-K(x_1-l_0)x_2 + \tau\,\dot{\theta}_s\right) - x_1^2\,\dot{\theta}_s\ddot{\theta}_s - x_1\,x_2\dot{\theta}_s^2\right)}{x_2}, \end{cases}$$

where $x_1 = l$ and $x_2 = \dot{l}$.

The other parameters of $r(\theta_r)$, ϕ and α, shown in Fig. 3, can be computed geometrically from *law of cosines* and *law of sines*:

$$\frac{l(\theta_s)}{\sin(\pi-\phi)} = \frac{R}{\sin(\alpha)} = \frac{r(\theta_r)}{\sin(\phi-\alpha)}, \tag{14}$$

$$l(\theta_s)^2 = r(\theta_r)^2 + R^2 - 2r(\theta_r)R\cos(\pi-\phi). \tag{15}$$

Substituting $r(\theta_r)$ from (14) in (15), yields:

$$l(\theta_s)^2 = \frac{\sin(\phi-\alpha)^2}{\sin(\phi)^2}\,l(\theta_s)^2 + R^2 + \frac{\sin(\phi-\alpha)}{\sin(\phi)}\,l(\theta_s)R\cos(\phi). \tag{16}$$

By some simple calculations, ϕ is determined as:

$$\phi = \cot^{-1}\left(\frac{l(\theta_s)\cos(\phi-\alpha) - R}{l(\theta_s)\sin(\phi-\alpha)}\right). \tag{17}$$

where $\cos(\phi-\alpha)$ and $\sin(\phi-\alpha)$ can be calculated from (8). Now, by substituting ϕ in (14), α and $r(\theta_r)$ can be calculated. Pair of $(\theta_r, r(\theta_r))$ defines geometrical shape of non-circular cam where $\theta_r = \theta_s + \alpha$.

B. Simplified Static Model

As the mass and the momentum inertia of roller are small, the dynamics of structure can be ignored; especially whenever the rotational velocity is constant or very slow. In such cases, $m\,a_R$, $m\,a_\theta$ and f_f are negligible. Considering this assumption, (13) is simplified as:

$$\frac{\mathrm{d}l(\theta_s)}{\mathrm{d}\theta_s} = \frac{\tau(\theta_s)}{K(l(\theta_s) - l_0)}. \tag{18}$$

Then, for any given profile of θ_s, parameters of a_R, a_θ, ω and f_f can be estimated from the dynamic equations.

III. Case Studies

To illustrate the design methodology, we realize some springs with different nonlinear profiles, as following:

$$\tau(\theta_s) = 0.3, \tag{19a}$$
$$\tau(\theta_s) = 0.02\,(\theta_s - 135)^3, \tag{19b}$$
$$\tau(\theta_s) = 0.15\,\tanh(\theta_s - 135), \tag{19c}$$
$$\tau(\theta_s) = 0.25\,\sin(2\,(\theta_s - 135)). \tag{19d}$$

These profiles are popular in the current applications of nonlinear spring; e.g. cubic profile is efficient in shock absorption in SEA or sinusoidal spring can be used for gravity compensation in manipulators. The design parameters are shown in Table I. All parameters are considered the same for all of above profiles. Due to oscillatory behaviour of spring, it is assumed that guide rotates with the sinusoidal time functionality:

$$\theta_s = -135\,\sin(\omega_s\,t + \frac{\pi}{2}) + 135. \tag{20}$$

For each profile, the designed cams are shown in Fig. 5 to Fig. 8, respectively where subfigures (a) show the prescribed torque angle profiles, subfigures (b) show the shape of designed cams, subfigures (c) show spring length and cam radius in the left figures and ϕ and $\phi - \alpha$ angles in the right figures and subfigures (d) show the normal and spring forces from left to right. The guide rotates counterclockwise from $\theta_s = 0$ to $\theta_s = 270$ degree. As it can be seen, the proposed method is cable of providing both positive and negative torques with just one cam. If the radius is increasing, which means $\dot{r} > 0$, the provided torque is positive, and whenever it is decreasing, i.e. $\dot{r} < 0$, the provided torque is negative.

A. Study of Design Parameters

In the case of static balance, the amount of provided torque is a function of the spring force, the spring length and the angle between the normal force and the spring force in each position. However, these variables are implicitly dependent on the initial configuration at position $\theta_s = 0$, namely the design parameters. To study the effects of these parameters, profile of cubic spring is designed for different sets of parameters. In Fig. 9a, the stiffness and initial deflection of spring are fixed. As it can be seen, the calculated profiles are similar and just scaled. Due to the simplified model (18), this is expected since $^{dl}/_{d\theta_s}$ is the function of total deflection, not just the rest length. In Fig. 9b, the stiffness and the rest length of spring are fixed. Here, the initial deflection is variable. In Fig. 9c, the rest length and the initial deflection of spring are fixed. In both the second and third cases, higher deflection or stiffness leads to lower variation of radius. Moreover, the provided torque is directly proportional to the spring stiffness for a pre-designed cam.

TABLE I
Design Parameters

Parameter	Value
Rest length of spring	$4\,cm$
Initial length of spring	$5\,cm$
Stiffness of spring	$5000\,^{N}/_{m}$
R^*	$7.5\,mm$
m^*	$3.85\,g$

*R and m are selected due to the off-the-shell miniature bearings.

B. Study of Dynamic Behaviour of the Proposed Structure

According to the dynamic model of the proposed structure, the designed cam is a function of the angular velocity; indeed, it seems that it behaves like a spring-damper. However, this dependency is ignorable due to small mass of roller, especially whenever the angular velocity is constant or very low. In such cases, the designed shape of cam is independent from angular velocities and easily simplified model can be used. In Fig. 10, the desired cubic torque-angle profile is compared to the generated torque for different angular velocity in the range of $0\,rpm$ to $120\,rpm$, which is the normal range of angular velocities in the robotics applications. As it can be seen, the error is less than 6% for velocities below $100\,rpm$. As a result, the damping behaviour is negligible in this range. For the angular velocity

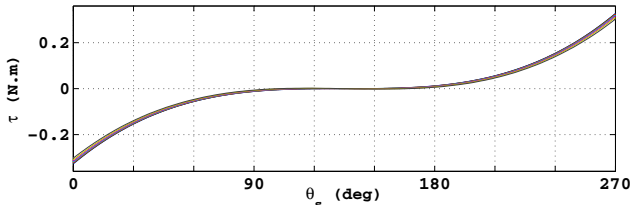

(a) Cubic torque profiles generated by a designed cam for different angular velocities,

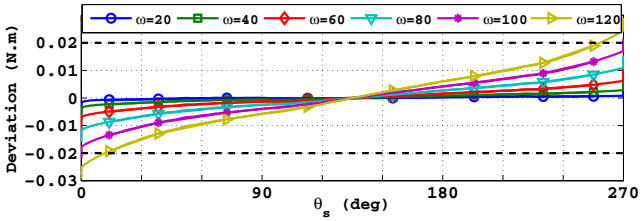

(b) Deviation of cubic torque profiles generated by a designed cam for different angular velocities,

Fig. 10. Comparison of the cam designing for the cubic spring with the dynamic model for different speeds, varying from $0\,rpm$ to $120\,rpm$.

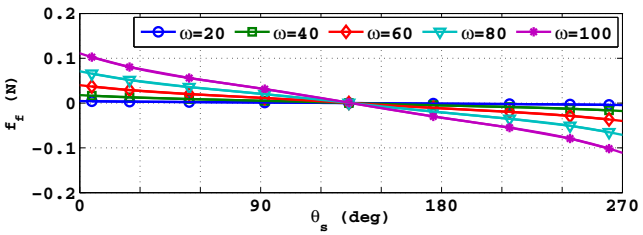

Fig. 11. Friction force in the cubic spring with different speeds in the range of 0 to $100 rpms$. Higher speed results in higher friction force.

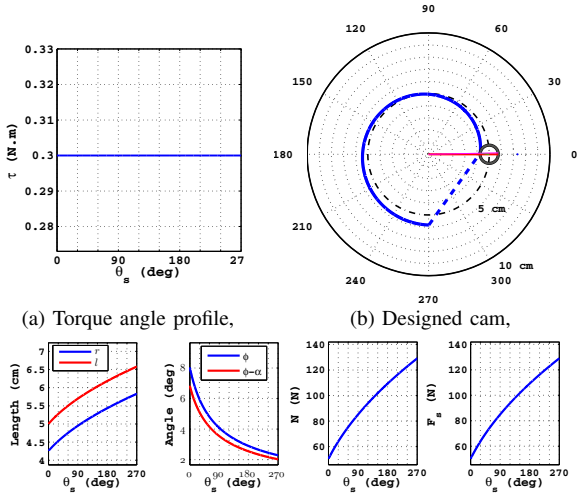

(a) Torque angle profile, (b) Designed cam,

(c) Geometry values, (d) Forces,

Fig. 5. Constant torque spring with profile of $\tau = 0.3$.

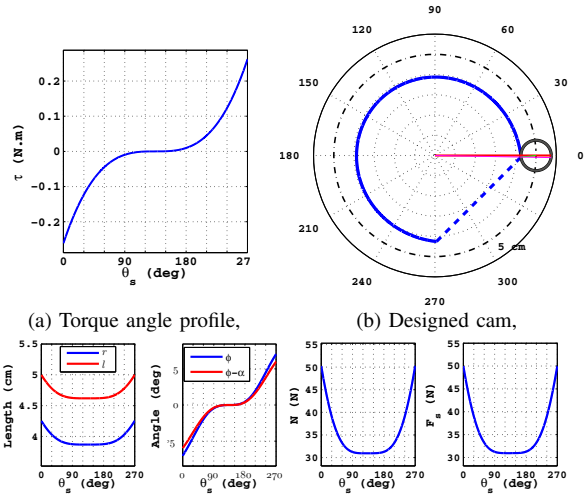

(a) Torque angle profile, (b) Designed cam,

(c) Geometry values, (d) Forces,

Fig. 6. Cubic spring with profile of $\tau = 0.02\,(\theta - 135)^3$.

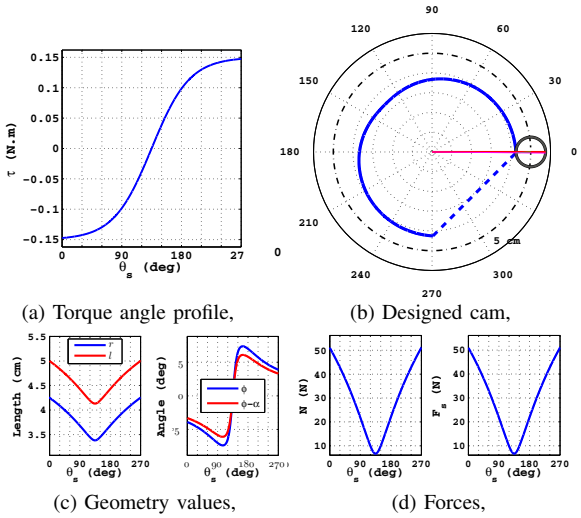

(a) Torque angle profile, (b) Designed cam,

(c) Geometry values, (d) Forces,

Fig. 7. Hyp. tangent spring with profile of $\tau = 0.15 \tanh(\theta_s - 135)$.

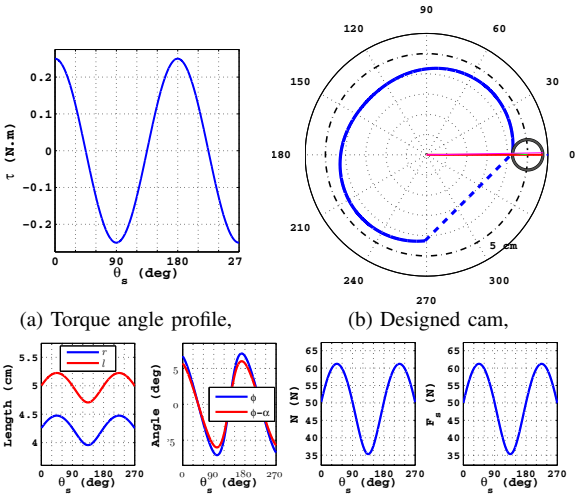

(a) Torque angle profile, (b) Designed cam,

(c) Geometry values, (d) Forces,

Fig. 8. Sinusoidal spring with profile of $\tau = 0.25 \sin(2(\theta_s - 135))$.

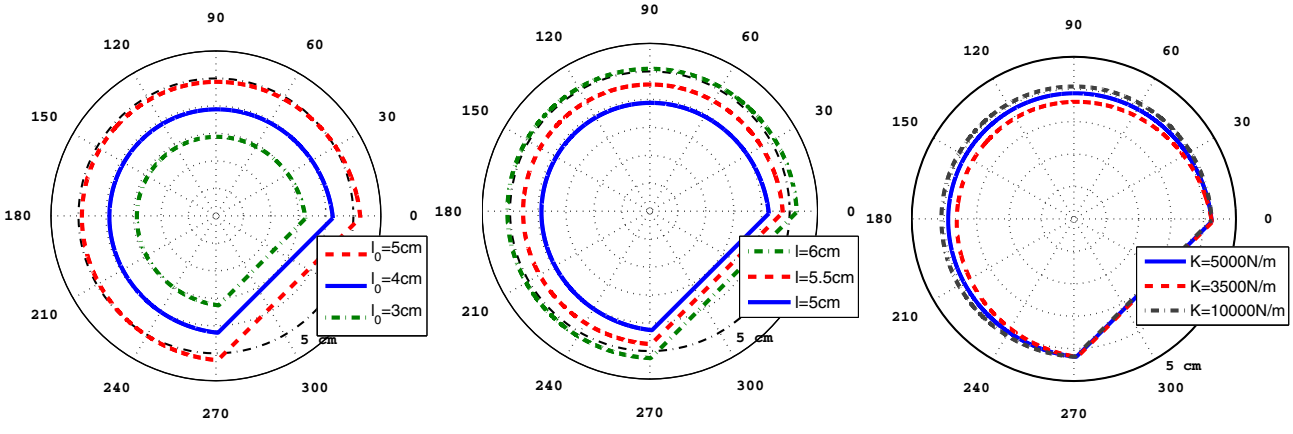

(a) (b) (c)

Fig. 9. Designed profiles of cubic spring for different sets of parameters. (a) Different rest lengths with fixed stiffness and initial deflection, (b) different initial deflections with fixed stiffness and rest length, (c) different stiffness with fixed rest length and initial deflection.

of $0\,rpm$, the simplified model is considered. Also, the friction force is shown for different angular velocities in Fig. 11 for the cubic spring. Due to the value of normal force, the friction force is always less than maximum static friction and so, the assumption of rolling without slipping is valid for all cases for any $\mu > 0.01$.

IV. Conclusion

In this paper, we proposed a new method for implementation of nonlinear spring, based on the combination of a linear spring with a nonlinear transmission mechanism. This method is capable of providing torque-angle profile with both positive and negative values with a single structure. The proposed structure consists of a non-circular cam, a roller which moves along outer circumference of the non-circular cam and a stretched linear spring, which is connected between center of the cam and center of the roller through a radial non-flexible guide. The cam is fixed and both spring guide and roller rotate along joint axis. We derived a set of differential equations in order to design the cam profile with for the exact model, considering the dynamics, and the simplified static model, ignoring the dynamics. By the proposed method, the cam of some popular nonlinear springs were designed, including constant, cubic, hyperbolic tangent and sinusoidal springs. Also, it was shown that both the exact and the simplified models have similar results for normal range of velocities. This structure is compact and can be coupled directly to a joint in various robotics applications; e.g. gravity compensation, actuator torque and power minimization, safe human-robot interactions and so on. As the future works, we are going to realize the structure and then develop it by adding some adaptable mechanism to realize a variable nonlinear spring.

Acknowledgement

The authors would like to acknowledge University of Tehran for providing supports for this research. The first author would also like to thank Atoosa Parsa for her comments on this article.

References

[1] J.-J. Park, B.-S. Kim, J.-B. Song, and H.-S. Kim, "Safe link mechanism based on passive compliance for safe human-robot collision," in *Robotics and Automation, 2007 IEEE International Conference on*, pp. 1152–1157, IEEE, 2007.

[2] N. Ulrich and V. Kumar, "Passive mechanical gravity compensation for robot manipulators," in *Robotics and Automation, 1991. Proceedings., 1991 IEEE International Conference on*, pp. 1536–1541, IEEE, 1991.

[3] G. A. Pratt and M. M. Williamson, "Series elastic actuators," in *Intelligent Robots and Systems 95.'Human Robot Interaction and Cooperative Robots', Proceedings. 1995 IEEE/RSJ International Conference on*, vol. 1, pp. 399–406, IEEE, 1995.

[4] M. Khoramshahi, A. Parsa, A. Ijspeert, and M. N. Ahmadabadi, "Natural dynamics modification for energy efficiency: A data-driven parallel compliance design method," in *2014 IEEE International Conference on Robotics and Automation (ICRA)*, pp. 2412–2417, IEEE, 2014.

[5] S. Maleki and M. N. Ahmadabadi, "Parallel spring simplifies actuator output torque and improves feed-forward learning," in *Robotics and Mechatronics (ICRoM), 2014 Second RSI/ISM International Conference on*, pp. 304–309, IEEE, 2014.

[6] M. H. H. Kani, M. Derafshian, H. J. Bidgoly, and M. N. Ahmadabadi, "Effect of flexible spine on stability of a passive quadruped robot: Experimental results," in *Robotics and Biomimetics (ROBIO), 2011 IEEE International Conference on*, pp. 2793–2798, IEEE, 2011.

[7] H. J. Bidgoly, A. Vafaei, A. Sadeghi, and M. N. Ahmadabadi, "Learning approach to study effect of flexible spine on running behavior of a quadruped robot," in *Proceeding of International Conference on Climbing and Walking Robots 2010, CLAWAR, pp. 11951201*, 2010.

[8] F. Iida and R. Pfeifer, "Cheap rapid locomotion of a quadruped robot: Self-stabilization of bounding gait," in *Intelligent Autonomous Systems*, vol. 8, pp. 642–649, 2004.

[9] R. M. Alexander, "Three uses for springs in legged locomotion," *The International Journal of Robotics Research*, vol. 9, no. 2, pp. 53–61, 1990.

[10] E. Suhir, "Shock protection with a nonlinear spring," *Components, Packaging, and Manufacturing Technology, Part A, IEEE Transactions on*, vol. 18, no. 2, pp. 430–437, 1995.

[11] G. Endo, H. Yamada, A. Yajima, M. Ogata, and S. Hirose, "A passive weight compensation mechanism with a non-circular pulley and a spring," in *Robotics and Automation (ICRA), 2010 IEEE International Conference on*, pp. 3843–3848, IEEE, 2010.

[12] B. Kim and A. D. Deshpande, "Design of Nonlinear Rotational Stiffness Using a Noncircular Pulley-Spring Mechanism," *Journal of Mechanisms and Robotics*, vol. 6, p. 041009, June 2014.

[13] D. Owaki and A. Ishiguro, "Enhancing stability of a passive dynamic running biped by exploiting a nonlinear spring," in *Intelligent Robots and Systems, 2006 IEEE/RSJ International Conference on*, pp. 4923–4928, IEEE, 2006.

[14] S. Wolf and G. Hirzinger, "A new variable stiffness design: Matching requirements of the next robot generation," in *Robotics and Automation, 2008. ICRA 2008. IEEE International Conference on*, pp. 1741–1746, IEEE, 2008.

[15] M. Khoramshahi, H. J. Bidgoly, S. Shafiee, A. Asaei, A. J. Ijspeert, and M. N. Ahmadabadi, "Piecewise linear spine for speedenergy efficiency trade-off in quadruped robots," *Robotics and Autonomous Systems*, vol. 61, no. 12, pp. 1350 – 1359, 2013.

[16] S. A. Migliore, E. A. Brown, and S. P. DeWeerth, "Biologically inspired joint stiffness control," in *Robotics and Automation, 2005. ICRA 2005. Proceedings of the 2005 IEEE International Conference on*, pp. 4508–4513, IEEE, 2005.

[17] N. Schmit and M. Okada, "Optimal design of nonlinear springs in robot mechanism: simultaneous design of trajectory and spring force profiles," *Advanced Robotics*, vol. 27, no. 1, pp. 33–46, 2013.

[18] J. Zawadzki and A. SIEMIEŃSKI, "Maximal frequency, amplitude, kinetic energy and elbow joint stiffness in cyclic movements," *Acta Bioeng. Biomech*, vol. 12, no. 2, pp. 55–64, 2010.

[19] T. P. Sapsis, D. D. Quinn, A. F. Vakakis, and L. A. Bergman, "Effective stiffening and damping enhancement of structures with strongly nonlinear local attachments," *Journal of vibration and acoustics*, vol. 134, no. 1, p. 011016, 2012.

[20] S. Yoon, N. Yazdi, J. Chae, N. Perkins, and K. Najafi, "Shock protection using integrated nonlinear spring shock stops," in *Micro Electro Mechanical Systems, 2006. MEMS 2006 Istanbul. 19th IEEE International Conference on*, pp. 702–705, IEEE, 2006.

[21] M. Okada and S. Kino, "Torque transmission mechanism with nonlinear passive stiffness using mechanical singularity," in *Robotics and Automation, 2008. ICRA 2008. IEEE International Conference on*, pp. 1735–1740, IEEE, 2008.

[22] K. F. Laurin-Kovitz, J. E. Colgate, and S. D. Carnes, "Design of components for programmable passive impedance," in *Robotics and Automation, 1991. Proceedings., 1991 IEEE International Conference on*, pp. 1476–1481, IEEE, 1991.

[23] C. V. Jutte and S. Kota, "Design of nonlinear springs for prescribed load-displacement functions," *Journal of Mechanical Design*, vol. 130, no. 8, p. 081403, 2008.

[24] T. Buhl, C. B. Pedersen, and O. Sigmund, "Stiffness design of geometrically nonlinear structures using topology optimization," *Structural and Multidisciplinary Optimization*, vol. 19, no. 2, pp. 93–104, 2000.

[25] N. Schmit and M. Okada, "Synthesis of a non-circular cable spool to realize a nonlinear rotational spring," in *Intelligent Robots and Systems (IROS), 2011 IEEE/RSJ International Conference on*, pp. 762–767, 2011.

[26] S. Sen and A. Bicchi, "A nonlinear elastic transmission for variable-stiffness-actuation: Objective and design," in *Proc. 15th National Conf. on Machine and Mechanisms, Chennai, Nov*.